J Mater Sci: Mater Med (2008) 19:2215–2222
DOI 10.1007/s10856-007-3323-z

# Nanoscale surface topography enhances cell adhesion and gene expression of madine darby canine kidney cells

**C. Y. Jin · B. S. Zhu · X. F. Wang · Q. H. Lu · W. T. Chen · X. J. Zhou**

Received: 31 May 2007 / Accepted: 2 November 2007 / Published online: 1 December 2007


**Abstract** Substrate topography is one of the key factors that influence cell behavior, such as cell attachment, adhesion, proliferation and differentiation. In the present work, nanostructures were produced on polystyrene Petri dish by polarized laser irradiation with the wavelength of 266 nm and the energy of 3.0 mJ/cm$^2$. Cell adhesion, growth and gene expression of Madine darby canine kidney (MDCK) cells cultured on smooth and nanogrooved substrates were investigated. The results indicated that cells preferred to adhere and grow on nanogrooved substrate. The distribution of cell cycle for cells on smooth substrates was different from that on nanogrooved substrate. The percentage of G1 phase cells on nanogrooved substrate (48.6 ± 1.4%) was lower than that on smooth substrate (57.6 ± 4.4%), while the percentage of cells on nanogrooved substrate in S (30.2 ± 0.5%) and G2/M (21.2 ± 1.1%) phase was higher than those on smooth substrate (25.1 ± 1.5% and 17.3 ± 3.3%, respectively). Moreover, the gene expression of cyclin D1 and keratin 18, which was examined by semi-quantitative reverse transcription polymerase chain reaction (RT-PCR), was significantly enhanced by nanogrooves, with an increase of cyclin D1 mRNA by 98% and an increase of keratin 18 mRNA by 75%. In conclusion, the nanogrooved surface features on polystyrene could alter cell cycle and enhance gene expression of cyclin D1 and keratin 18 in MDCK cells, which partly explained the increased cell adhesion and growth on nanogrooved substrate.

C. Y. Jin
Instrumental Analysis Center and School of Chemistry & Chemical Engineering, Shanghai Jiao Tong University, Shanghai 200240, China

B. S. Zhu
Instrumental Analysis Center, Shanghai Jiao Tong University, Shanghai 200240, China

X. F. Wang
School of Life Science and Biotechnology, Shanghai Jiao Tong University, Shanghai 200240, China

Q. H. Lu (✉)
School of Chemistry & Chemical Engineering, Shanghai Jiao Tong University, Shanghai 200240, China
e-mail: qhlu@sjtu.edu.cn

W. T. Chen · X. J. Zhou
Ninth People's Hospital, School of Medicine, Shanghai Jiao Tong University, Shanghai 200011, China

## 1 Introduction

In the fields of biomedical engineering and tissue engineering, cell–substrate interactions are dependent on chemical and physical properties of material surfaces, which modulate cell adhesion, morphology and cytokine production [1, 2]. In vivo, cells are living in a complex environment, which is composed of pores, fibers and ridges at nanometer scale. Cells are sensitive to these nanostructures. For example, epithelial cells rest upon a specialized extracellular matrix (ECM), known as basement membrane, which not only provides biochemical stimuli, but also presents an intricate, three-dimensional meshwork to regulate cell behavior and function [3–5]. Therefore, it is necessary to design and fabricate substrates with micro- or nanostructures, which can be used to mimic ECM and study cell–substrate interactions. Several methods, such as photo-immobilization [6], microcontact printing [7], electronspinning [8, 9], electron-beam lithography [10] and inkjet printing [11], have been applied to produce micro- or nanostructures on substrate surfaces, and many types of cells have been studied.

Cell responses to topography of biomaterials are dependent not only on cell types but also on cell–cell interactions [12, 13]. Madine darby canine kidney cell (MDCK) is a type of renal distal tubule epithelial cell line and often used to study important and fundamental issues in epithelial cell biology [14]. MDCK cells incline to form an epithelial tight junction monolayer, which is composed of different membrane receptors and iron transporters for kidney homeostatic control. Curtis and Wilkinson found that when MDCK cells were cultured on microgrooved substrate, the phenomenon of microgrooves contact guiding cell alignment disappeared, which was mainly due to cell–cell interactions overriding the effect of topography of the substrate on cell behavior [12, 15]. Our previous studies have showed that laser-irradiated nanogrooved could guide rat glioma C6 cell alignment [16]. However, epithelial cell–nanogroove interactions are still unknown and fundamental investigations need to be done.

Epithelial cell adhesion to basement membrane or substrate is a prerequisite for cell growth and survival. Adhesion is related to cell cycle, which enables cells pass G1 phase to S phase. The transition rate of cell cycle progression is largely determined by gene expression of cyclin D1 [17]. Moreover, epithelial cell adhesion to substrate is mediated by hemidesmosome, which is served as an anchorage site connecting to keratin cytoskeleton [18]. The expression of keratin 18 is suggested to be a primary expression in epithelia. Thus, the investigation of expression of cyclin D1 and keratin 18 mRNA will help us to understand the possible mechanisms of MDCK cell adhesion at molecular level.

In this work, we focused on the influence of laser-irradiated nanogrooves on polystyrene (PS) substrates on cell adhesion, cell cycle and gene expression. PS was chosen because it is widely used as substrates in cell and tissue culture in vitro. The periodicity and depth of nanogrooves could be precisely controlled by changing the incident angle of laser. Laser irradiation can provide an exact, simple, cost-effective technique to fabricate a large area with nanogrooved structures. MDCK cell adhesion and growth were tested with phase contrast microscopy, MTT assay and flow cytometry. The specific gene expressions of cyclin D1 and keratin 18 were measured with semi-quantitative RT-PCR.

## 2 Materials and methods

### 2.1 Fabrication of nanogrooves and micropatterned substrates

Nanogrooves were fabricated on PS surfaces by direct laser irradiation. The smooth PS tissue culture Petri dishes (Gongdong Co., China) were irradiated with the pulse polarized UV-laser ($\lambda = 266$ nm), generated by the Nd: YAG laser (GCR-4, Contimuum Electro-Optics, Inc., Co.). The repetition rate was 10 Hz and the duration time was 5 ns. The samples were fixed on a moving X–Y platform (MA 505 Physik Instrumente, Germany), which was controlled by a computer with the speed of 0.001 mm/s in the X direction and 10 mm/s in the Y direction. The irradiation energy was 3 mJ/cm$^2$. The laser incident angle was changed from 0° to 35°. The samples were characterized by atomic force microscopy (AFM, Multimode Nanoscope III, Digital Instrument) in contact mode. The periodicity and depth of nanogrooves were measured by AFM section images.

A micropatterned substrate for cell adhesion analysis was prepared by laser irradiation with a photofilm mask, which was fabricated with regular microdomained arrays with $CO_2$-pulsed laser marker (Hans Laser Technology Co., China). The diameter of the domains was about 50 μm, and the distance between domains was about 70 μm.

The nanogrooved Petri dishes and 96-well tissue culture plates were produced with the laser incident angle of 25°.

### 2.2 Cell culture

MDCK cells (obtained from the Cell Bank of Shanghai Institutes for Biological Sciences, Chinese Academy of Science, China) were cultured in high sugar Dulbecco's modified Eagle's medium (DMEM, Gibco), supplemented with 10% fetal bovine serum (FBS, Hyclone), 100 U/mL penicillin and 100 μg/mL streptomycin (Sangon, China) at 37°C in an atmosphere with 5% $CO_2$. The medium was changed every 2 days.

### 2.3 Cell adhesion and MTT assays

Cells were seeded at a concentration of $2.5 \times 10^4$ cells/cm$^2$ on a micropatterned substrate and cultured for 36 h. Cell adhesion of living cells on the substrates was observed with a phase contrast microscope (TE2000-S, Nikon), and the picture was taken by a Digital camera (Coolpix 4500, Nikon).

MTT assay was used to evaluate MDCK cell growth on smooth and nanogrooved substrates. Mitochondrial enzymes in alive cells can decompose a tetrazollium salt, 3-(4,5-dimethyldiazol-2-yl)-2,5 diphenyl tetrazolium bromide (MTT), to a colored formazan product. The cells were seeded into 96-well tissue culture plates with a density of 5,000 cell/well. After the cells were cultured for 2 days, 20 μL of a 5 mg/mL solution of MTT in 0.01 M PBS was

added to each well, and the cells were cultured at 37°C for another 4 h. Then the medium was carefully removed and the purple products were dissolved in 0.2 mL of dimethyl sulfoxide (DMSO). The plates were shaken for 10 min and the optical density (OD) of the dissolved solute was measured by an ELISA reader (BP 800 Biohit) with a light of 490 nm wavelength. Each sample was repeated for three times and the data were shown by mean ± standard derivation (SD). Wells without nanogrooves were served as the control.

### 2.4 Cell morphology and actin cytoskeleton

Cells were seeded at a concentration of $2.5 \times 10^4$ cells/cm$^2$ and cultured on PS coated glass coverslips for 24 h. The cells were fixed in 2% glutaraldehyde in 0.01 M PBS for 10 min, washed in 0.01 M PBS, and permeabilized with 0.2% Trion X-100 in 0.01 M PBS for 5 min. After being washed for three times in PBS, the cells were incubated in FITC-phalloidin (Sigma-Aldrich) solution (1:40 in diluted 0.01 M PBS) for 40 min, and rinsed in 0.01 M PBS. Specimens were mounted onto slides and sealed with glycerin and examined with confocal laser scanning microscopy (CLSM, Leica TCS SP2).

### 2.5 Cell cycle analysis

MDCK cells were seeded at a density of $2.5 \times 10^4$ cells/cm$^2$ on smooth and nanogrooved substrates and cultured for 2 days. The cells were harvested, washed in ice-cold PBS, fixed in 70% ethanol for 1 h on ice, rinsed with PBS, and stained with propidium iodide (50 μg/mL) and RNAase (10 μg/mL) for 30 min at room temperature. Cell cycle was analyzed by flow cytometry (FACS Calibur, Becton Dicknson), and the percentage of cells in the various phases of cell cycle was calculated using Cell Fit software. The experiments were repeated for three times, and the data were shown by mean ± SD.

### 2.6 Cyclin D1 and keratin 18 expression

The expression of cyclin D1 and keratin 18 in MDCK cells were examined by the semi-quantitative reverse transcriptase-polymerase chain reaction (RT-PCR). Cells were seeded at a concentration of $2.5 \times 10^4$ cells/cm$^2$ on smooth and nanogrooved substrates. The total RNA was extracted with 1 mL of Trizol (Invitrogen) according to the protocols. Briefly, the cells were homogenized and solubilized in a chloroform solution at 4 °C. Supernatants were obtained by centrifugation and then added 500 μL of isopropanol at 4°C for 30 min. The precipitates were washed with cold 75% ethanol. Finally, the RNA pellets were dissolved in 0.01% DEPC water and preserved at −40 °C. Single-stranded cDNA was obtained by reverse transcription of 3 μL of the total RNA using oligo dT, according to the guidelines of manufacturer. The reaction mixtures were incubated at 42 °C for 2 h, and excess of enzyme was inactivated at 95 °C for 5 min. The resulting cDNAs were stored at −40°C for subsequent analysis.

**Table 1** Oligonucleotide primers for gene expression analysis by RT-PCR

| Gene | Target cDNA primer sequence (forward/reverse5′ to 3′) | Expected product size (bp) |
|---|---|---|
| Cyclin D1 | 5′-GCC ATG ACC CCA CAC GAC-3′ | 291 |
| | 5′-ACT CCA GCA GGG CTT CGA T-3′ | |
| Keratin 18 | 5′-GGA GGT CGA GAC CCG CTA C-3′ | 201 |
| | 5′-GCT GTC CAG GGC GTC AGT A-3′ | |
| GAPDH | 5′-CATGACCACTGTCCATGCCA-3′ | 279 |
| | 5′-CATCAAAGGTGAAAGAATGGGTG-3′ | |

The RT-PCR analysis was performed with RT-PCR kit (RNA-PCR kit, BioDev, China) according to the instruction. Briefly, the reaction mixture (25 μL) contained 1 μL of RT reaction products, 12.5 μL of Premix *Taq* polymerase (Takara Biomedicals, China), 10.5 μL of sterilized water, and 1 μL of sense and antisense primers for cyclin D1, keratin 18 and glyceraldehyde-3-phosphate dehydrogenase (GAPDH). The PCR amplification was performed by polymerase chain reaction for 33 cycles with specific primers for keratin 18, cyclin D1 and GAPDH (Table 1). The thermocycling conditions were 95 °C for 30 s, 58 °C for 30 s, 72 °C for 1 min for all PCRs, then extended at 72 °C for 10 min. The reaction products were then separated by electrophoresis on a 1% agarose gel in Tris–Acetic acid–EDTA (TAE) buffer and stained by ethidium bromide and analyzed with a fluorescence imaging analyzer (DH-2 Digital Imaging Systems, HUADIAN, China). The 100 bp DNA of ladder marker (Takara Biomedicals, China) was used and the gene expression in different probes was evaluated semiquantitatively. The GAPDH-activity was adjusted in the different specimens. The final numeric values were calculated in ratio of cyclin D1 and keratin 18 to GAPDH and analyzed using TotalLab v2005 software. The experiments were repeated for four times, and the data were shown by mean ± SD.

### 2.7 Statistical analysis

The data presented in this work were the typical results of at least three separate experiments. A Student's *t*-test was

used to examine the differences between nanogrooved and smooth substrates. A value of $P < 0.05$ was considered statistically significant and the results were presented as mean ± SD.

## 3 Results

### 3.1 Surface topography

Four types of PS substrates were characterized by AFM in contact mode (Fig. 1a–d). PS culture Petri dish (Fig. 1a) was a control substrate. The periodic nanogrooves (Fig. 1b, 3D section) were formed on laser-irradiated PS substrates. The periodicity of the nanogrooves structure could be well controlled at the range of 300–400 nm. The periodicity ($\Lambda$) is related to the wavelength ($\lambda$) and the incident angle of laser ($\theta$), and the apparent refractive index of a material ($n$), which can be described by the following formula [19]:

$$\lambda/\Lambda = n - \mathrm{Sin}\theta$$

However, non-continuous nanogrooves (Fig. 1c) and melted nanodots (Fig. 1d) appeared on the laser-irradiated

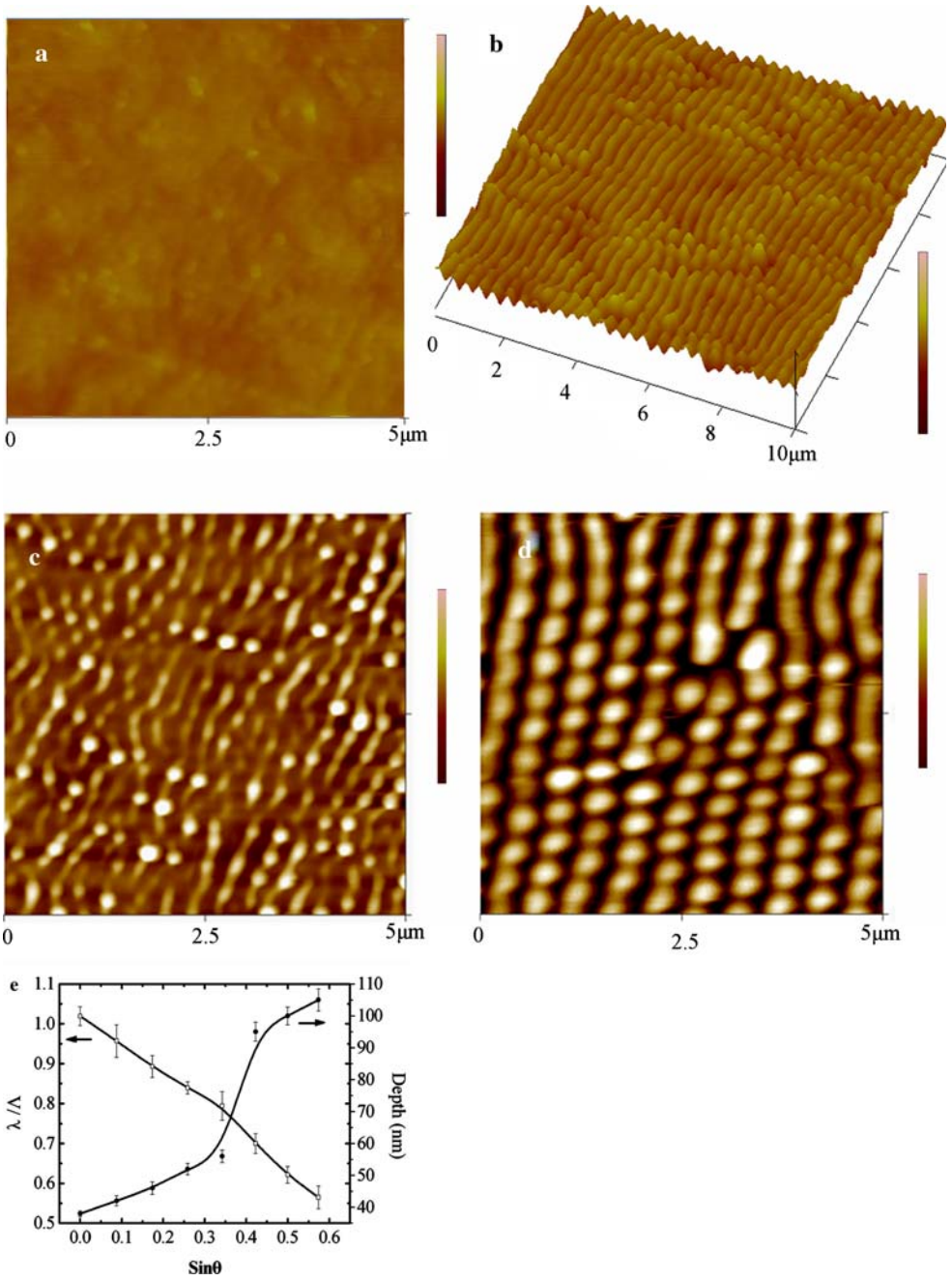


**Fig. 1** AFM images of four types of polystyrene substrates: (**a**) cell culture Petri dish, (**b**) continuous nanogrooves with the periodicity from 300 nm to 400 nm, (**c**) non-continuous nanogrooves, and (**d**) melt nanodots. (**e**) Periodicity and depth of continuous nanogrooves controlled by laser incident angle ($\Lambda$: the periodicity, $\lambda$: wavelength of laser, $\theta$: incident angle). Bar: 200 nm

substrates when the laser incident angle was below 10° or above 35°. When the laser irradiation energy was fixed, the depth of nanogrooves was also influenced by the incident angle of laser, forming the depth change from 40 nm to 90 nm (Fig. 1e).

### 3.2 Cell adhesion and growth

To investigate cell adhesion on smooth and nanogrooved substrates, MDCK cells were seeded on a micropatterned substrate with smooth and laser-irradiated domains. After culturing for 36 h, cells were observed with a phase contrast microscope (Fig. 2). The cells in nanogrooved domains (in circles) were inclined to form sheets and colonies, and adhered firmly, which made them difficult to be removed by rinsing force. However, the cells adhered weakly in the smooth space (outside of circles) were round, isolated, and easy to be rinsed away.

Cell growth on smooth and nanogrooved substrates was evaluated by a MTT assay. Cells were cultured for 1, 2, 3, 4 and 5 days, respectively. MTT result showed that the cells on nanogrooved substrate grew faster than those on smooth substrate (Fig. 3a). The OD value of MDCK cells on nanogrooved substrates reached the maximum on the 4th day, which was double that on smooth substrates. On the 5th day, the OD value of cells on smooth and nanogrooved substrates started to decrease, which might be due to the apoptosis of some cells.

The influence of the periodicity of nanogrooves on cell growth was also investigated by a MTT assay. The OD value of cells increased with the increase of the periodicity of nanogrooves ranged from 280 nm to 380 nm, and then

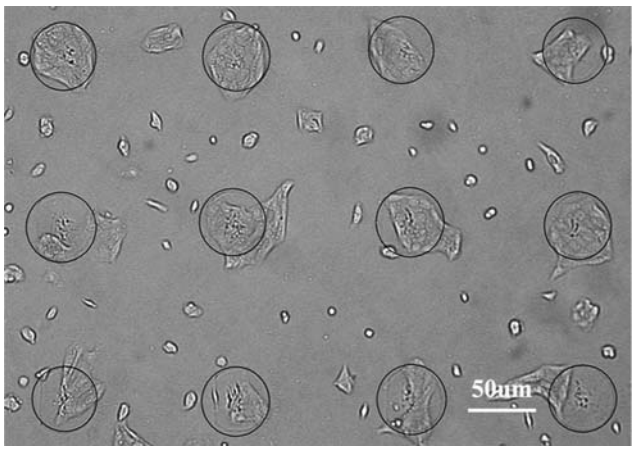


**Fig. 2** A phase contrast microscopy image of MDCK cells cultured for 36 h on a micropatterned substrate with the diameter of laser-irradiated domain of 50 μm, and the space between domains of 70 μm. Bar: 50 μm

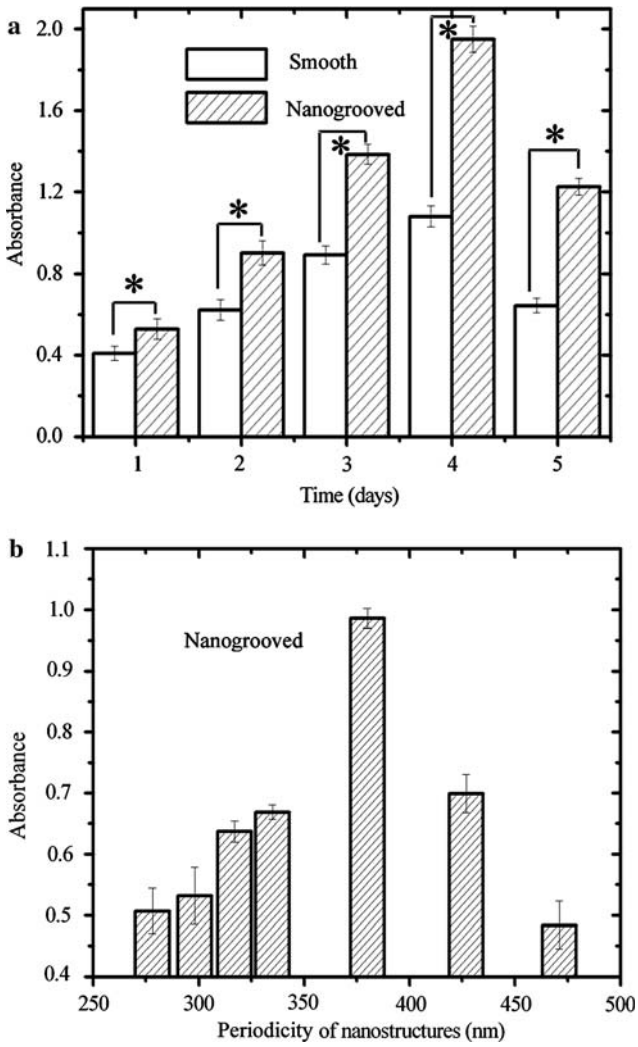


**Fig. 3** (**a**) Cell growth on smooth and nanogrooved substrates for 1, 2, 3, 4 and 5 days evaluated by a MTT assay. * $p < 0.05$. (**b**) Cell growth affected by the periodicity of nanogrooves. Absorbance of cells cultured on nanogrooves increased with the periodicity ranged from 280 nm to 380 nm, and then decreased when the periodicity exceeded 380 nm

decreased due to the rupture of the periodic nanogrooves when the periodicity exceeded 380 nm (Fig. 3b). It indicated that nanodots or non-continuous nanogrooves could not accelerate cell growth, which also has been reported by other group [20].

Cell morphology on smooth and nanogrooved substrates was examined with a confocal microscope. The cells cultured on smooth substrate were round and the distribution of the actin filaments was irregular (Fig. 4a). In contrast, the cells on nanogrooved substrate spread well and cluster-like actin assemblies were found to rearrange and orient along the direction of the periodic nanogrooves (Fig. 4b).

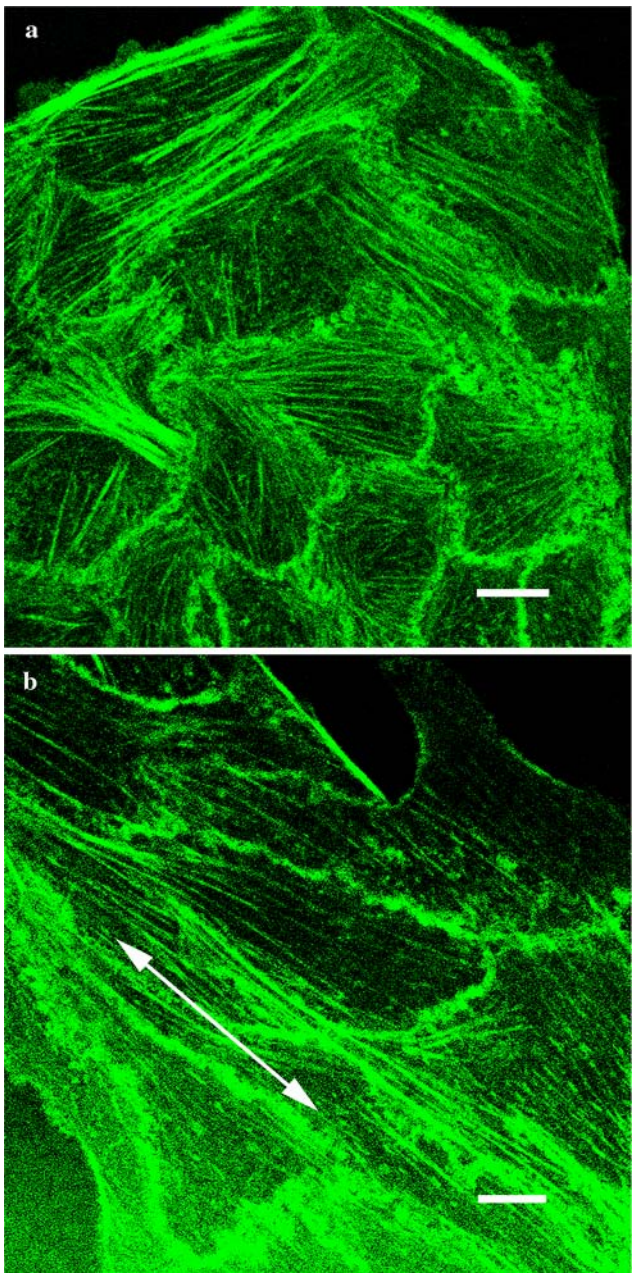


**Fig. 4** Distribution of actins in MDCK cells cultured on smooth (**a**) and nanogrooved (**b**) substrates examined with confocal laser scanning microscopy. (**a**) The cells were round and actin filaments were irregular. (**b**) The cells were larger and the actin filaments oriented along the direction of the ridges/grooves. The arrow in (**b**) indicated the direction of the ridges/grooves. The cells were stained with FITC-phalloidin. Bar: 10 μm

### 3.3 Cell cycle analysis

Cell cycle of MDCK cells cultured on smooth and nanogrooved substrates was analyzed by DNA content using flow cytometry (Fig. 5). The percentage of cells in G0/G1, S, G2/M phase was calculated, which was based on DNA content distribution histogram. The results displayed that

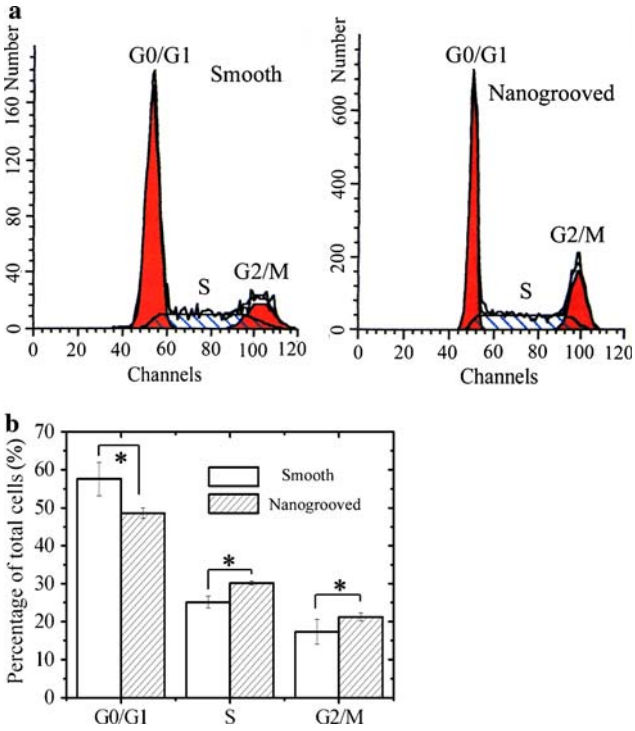


**Fig. 5** The cell cycle of MDCK cells cultured on smooth and nanogrooved substrates for 48 h analyzed by flow cytometry. (**a**) A histogram of the DNA content of cells. (**b**) The percentage of total cells in each phase of the cell cycle. The cells were stained with propidium iodide. * $p < 0.05$

the percentage of cells on nanogrooved substrates in G1 phase (48.6 ± 1.4%) was lower than that on smooth substrates (57.6 ± 4.4%). However, the percentage of cells on nanogrooved substrates in S phase (30.2 ± 0.5%) and that in G2/M phase (21.2 ± 1.1%) were higher than those on smooth substrates (25.1 ± 1.5% and 17.3 ± 3.3%, respectively).

### 3.4 Gene expression of cyclin D1 and keratin 18 mRNA

Gene expression of cyclin D1 and keratin 18 in MDCK cells cultured on smooth and nanogrooved substrates was analyzed by semi-quantitative RT-PCR. Cyclin D1 is one of cell cycle-related genes, which is related to cells in G1 phase entering into S phase. Keratin 18 gene plays an important role in epithelial cell adhesion. RT-PCR analysis revealed that both the content of cyclin D1 (Fig. 6a) and that of keratin 18 (Fig. 6b) in cells on nanogrooved substrate was different from those on smooth substrate. Further semiquantitative analysis indicated that content of cyclin D1 (98%) and that of keratin 18 (75%) in cells on nanogrooved substrate were higher than those on smooth substrate (Fig. 6c).

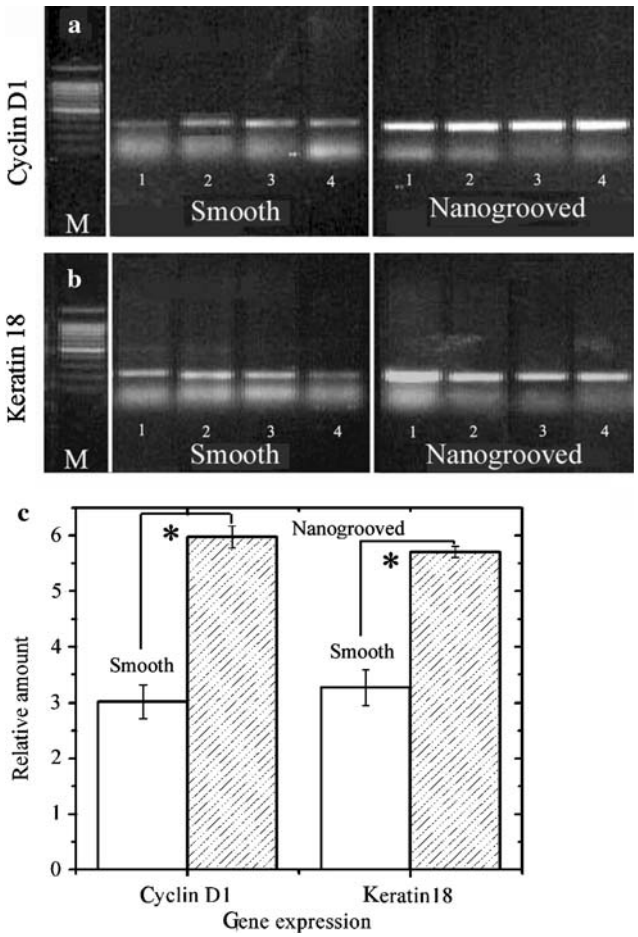


**Fig. 6** Gene expression of cyclin D1 mRNA (291 bp) (**a**) and keratin 18 mRNA (201 bp) (**b**) in MDCK cells cultured on smooth and nanogrooved substrates for 48 h examined with semi-RT-PCR. The marker (M) was 100 bp DNA ladder. (**c**) The relative amount of cyclin D1 and keratin 18 expression to GAPDH analyzed with TotalLab v2005 software. The experiments were repeated for four times, and the data were shown by mean ± SD. * $p < 0.05$

## 4 Discussion

Surface topography of an implant material is one of factors that determine its biocompatibility [21]. One of strategies in mimicking ECM is to modify substrate surfaces with micro- or nanometer scale features, which could provide an initial support for cell adhesion, and accelerate to form functional tissues. The mechanisms of influence of nanoscale topography on cell behavior are still unknown. Several possible hypotheses in subtle surface features inducing cell behavior changes have been proposed. Some researchers suggested that the conformation of adsorbed proteins could influence cell adhesion and ECM formation [22–24]. Others found that the integrins, a superfamily of cell surface receptors with $\alpha$- and $\beta$-subunits, could modulate cell–cell and cell–substrate interactions. The integrin-mediated cell adhesion to the substrate directed formation of hierarchical adhesive complexes and focal adhesions [25, 26]. However, Gallant and his co-workers believed that cell adhesion strength appeared to be regulated by an amount of localized structural proteins in the cytoskeleton, which were recruited for forming focal adhesion [27]. All these viewpoints have suggested that integrin binding, focal adhesion assembly and adhesive area affected cell adhesion to biomaterial surfaces. The present work attempted to explain the mechanism of nanogrooves affecting cell adhesion and growth at the molecular level.

In this work, laser irradiation was successfully applied to produce nanogrooves on PS substrates. The cell–nanogroove interactions played an important role in determining cell behavior. When cells were seeded onto the nanogrooved substrate, nanogrooves might direct initial cell adhesion, cell cycle progression, and the specific gene expression through numerous signal pathways. Focal adhesion could mediate or transfer surface cues and signals to affect the reorganization of actin cytoskeleton and the generation of membrane protrusions and traction forces.

MDCK cells, an epithelial cell line, polarize in response to adhesive contacts with basement membrane and tight junctions with neighboring cells in vivo [28]. When culturing on a micropatterned substrate, MDCK cells became colonies and islands with favorable adhesion and growth in nanogrooved domains in Fig. 2, which also showed that MDCK cells still maintained their apical-basolateral functional polarity. It would have potential application in patterning cells on substrate surfaces [29, 30]. Quantitative evaluation of MTT results indicated that suitable periodicity of nanogrooves could promote cell growth. Cell cycle analysis suggested that nanogrooved substrate influenced cell cycle progression by accelerating cells in G1 phase to enter S phase. The prominent gene expression of cyclin D1, which was related to cell cycle, confirmed that cell growth was modulated by subtle surface features. In some studies, over expression of cyclin D1 was considered as a marker of cancer [31]. Nevertheless, the appropriate enhancement of cyclin D1 mRNA expression was helpful for cell growth.

Hemidesmosomes and focal adhesions are major cell–matrix adhesions of epithelial cells [32]. In hemidesmosomes, integrin is connected to intermediate filaments-keratin [18]. Co-polymers of the type II keratin 8 and type I keratin 18 form the major intermediate filament network in epithelia [33–35], and keratin 18 is a particular gene expression of normal kidney [36–38]. Thus, we chose keratin 18 to study the influence of nanogrooved substrate on cell adhesion. The enhanced keratin 18 mRNA gene expression revealed that nanogrooves could stimulate the formation of hemidesmosomes. Moreover, it also showed that MDCK cells cultured on nanogrooved substrate still maintained their polar organization of epithelial cells,

although there were some elongated actin filaments in MDCK cell colonies (Fig. 4).

## 5 Conclusion

In conclusion, laser-irradiated nanogrooves on PS substrate could promote MDCK cell adhesion and growth, as well as gene expression of cyclin D1 and keratin 18. These results suggested that the changed cell behavior on nanogrooved substrate might be via initial adherence and subsequent actin rearrangement, which was related to cell cycle progression and hemidesmosomes formation. These findings would be helpful for understanding the mechanisms of cell behavior regulated by nanogrooves at the molecular level.

**Acknowledgements** This work was supported by the National Natural Science Foundation of China (No. 60577049 and 30572053), "Kua Shi Ji Program" of the Ministry of Education of China, and a Fundamental Key Project (No. 05JC14019) of the Science and Technology Commission of Shanghai Municipal Government.

## References

1. K. MATSUZAKA, M. YOSHINARI, M. SHIMONO and T. INOUE, *J. Biomed. Mater. Res.* **68A** (2004) 227
2. A. ANDERSSON, F. BACKHED, A. V. EULER, A. R. DAHLFORS, D. SUTHERLAND and B. KASEMO, *Biomaterials* **24** (2003) 3427
3. D. M. BRUNETTE, *Exp. Cell Res.* **164** (1986) 11
4. G. A. DUNN and A. F. BROWN, *J. Cell Sci.* **83** (1986) 313
5. A. CURTIS and C. WILKINSON, *Trends Biotechnol.* **19** (2001) 97
6. T. KONNO, H. HASUDA, K. ISHIHARA and Y. ITO, *Biomaterials* **26** (2005) 1381
7. K. E. SCHMALENBERG and K. E. UHRICH, *Biomaterials* **26** (2005) 1423
8. CH. H. KIM, M. S. KHIL, H. Y. KIM, H. U. LEE and K. Y. JAHNG, *J. Biomed. Mater. Res.* **78B** (2006) 283
9. Y. ZHU, M. F. LEONG, W. F. ONG, M. B. CHAN-PARK and K. S. CHIAN, *Biomaterials* **28** (2007) 861
10. A. I. TEIXEIRA, G. A. MCKIE, J. D. FOLEY, P. J. BERTICS, P. F. NEALEY and C. J. MURPHY, *Biomaterials* **27** (2006) 3945
11. S. ILKHANIZADEH, A. I. TEIXEIRA and O. HERMANSON, *Biomaterials* **28** (2007) 3936
12. P. CLARK, P. CONNOLLY, A. S. G. CURTIS, J. A. T. DOW and C. D. W. WILKINSON, *J. Cell Sci.* **99** (1991) 73
13. A. ANDERSSON, J. BRINK, U. LIDBERG and D. S. SUTHERLAND, *IEEE T. Nanobiosci.* **2** (2003) 49
14. K. SIMONS and S. D. FULLER, *Annu. Rev. Cell Biol.* **1** (1985) 243
15. P. CLARK, P. CONNOLLY, A. S. G. CURTIS, J. A. T. DOW and C. D. W. WILKINSON, *Development* **108** (1990) 635
16. B. S. ZHU, Q. Q. ZHANG, Q. H. LUA, Y. H. XU, J. YIN, J. HU and Z. G. WANG, *Biomaterials* **25** (2004) 4215
17. G. RADEVA, T. PETROCELLI, E. BEHREND, C. LEUNGHAGESTEIJN, J. FILMUS, J. SLINGERLAND and S. DEHAR, *J. Biol. Chem.* **272** (1997) 13937
18. L. FONTAO, J. STUTZMANN, P. GENDRY and J. F. LAUNAY, *Exp. Cell Res.* **250** (1999) 298
19. M. CSETE and Z. BOR, *Appl. Surf. Sci.* **133** (1998) 5
20. M. J. DALBY, S. CHILDS, M. O. RIEHLE, H. J. H. JOHNSTONE, S. AFFROSSMAN and A. S. G. CURTIS, *Biomaterials* **24** (2003) 927
21. S. J. LEE, J. S. CHOI, K. S. PARK, G. KHANG, Y. M. LEE and H. B. LEE, *Biomaterials* **25** (2004) 4699
22. T. HASEGAWA, H. OGUCHI, M. MIZUNO and Y. KUBOKI, *Jpn. J. Oral. Biol.* **36** (1994) 383
23. R. T. GETTENS, Z. BAI and J. L. GILBERT, *J. Biomed. Mater. Res.* **72**(A) (2005) 246
24. C. W. SUH, M. Y. KIM and J. B. CHOO, *J. Biotechnol.* **112** (2004) 67
25. R. L. JULIANO and S. HASKILL, *J. Cell Biol.* **120** (1993) 577
26. C. RENNER, B. SACCA and L. MORODER, *Biopolymers* **76** (2004) 34
27. N. D. GALLANT, K. E. MICHAEL and A. J. GARCIA, *Mol. Biol. Cell* **16** (2005) 4329
28. K. S. MATLIN, B. HAUS and A. ZUK, *Methods* **30** (2003) 235
29. G. KUMAR, Y. C. WANG, C. CO and C. C. HO, *Langmuir* **19** (2003) 10550
30. S. LAN, M. VEISEH and M. Q. ZHANG, *Biosen. Bioelectro.* **20** (2005) 1697
31. J. DING, R. H. ZHANG, J. X. LI, C. F. XUE and C. S. HUANG, *Mol. Cell. Biochem.* **287** (2006) 117
32. D. TSURUTA, S. B. HOPKINSON and J. C. R. JONES, *Cell Motil. Cytoskel.* **54** (2003) 122
33. P. A. COULOMBE and P. WONG, *Nat. Cell Biol.* **6**(8) (2004) 699
34. H. HERRMANN and U. AEBIANNU, *Rev. Biochem.* **73** (2004) 749
35. D. DEPIANTOA and P. A. COULOMBE, *Exp. Cell Res.* **301** (2004) 68
36. A. WASEEM, U. KARSTEN, I. M. LEIGH, P. PURKIS, N. H. WASEEM and E. B. LANE, *Biochemistry* **43** (2004) 1283
37. S. YAMADA, D. WIRTZ and P. A. COULOMBE, *J. Struct. Biol.* **143** (2003) 45
38. R. WINFRIED, H. ALESSANDRA, M. NIMA, X. F. FRANZ and A. JUDITH, *Med. Pediatr. Oncol.* **37** (2001) 357